

Generation and protection of Maximally Entangled State between many modes in an optical network with dissipation

Raul Coto and Miguel Orszag

Instituto de Física, Pontificia Universidad Católica de Chile, Casilla 306, Santiago, Chile

Vitalie Eremeev

Facultad de Ingeniería, Universidad Diego Portales, Santiago, Chile

(Dated: May 10, 2016)

We present a three-cavity network model with two modes in each cavity and a non-linear medium that generates a Kerr type interaction via both self-phase and cross-phase modulation processes. We have two main goals. The first one is to generate a multipartite Maximally Entangled State (MES), starting from the ground state of the system. We address the problem both without and with dissipation. Secondly, we want to protect the MES from decoherence. While studying the MES, we analyze different bipartite and multipartite entanglement measures. We also study the effect of an Avoided Level Crossing (ALC) identified by the critical behavior of the entanglement measures, thus showing that the quantum correlations act as a witness for such phenomena. Our findings provide the quantum tools to perform the operation of generation and protection of a maximally entangled state in a cavity QED environment.

PACS numbers:

I. INTRODUCTION

At the present time, quantum entanglement [1] is still the most common and efficient resource [2] for quantum information, computation and communication tasks, thus it is highly desirable to operate with maximally entangled states, which can be realized in a variety of setups [1, 3, 4]. Hence, quantum protocols used for generation, protection and communication of the Maximally Entangled State (MES) are in the continuous development and improvement, even considering that during the last decade, alternative resources, such as quantum discord, have been put forward and studied theoretically as well as experimentally [5–7].

Furthermore, all non-classical correlations can be activated into distillable entanglement and recently it has been shown that one can generate entanglement from classical correlations via local dissipation [8–12].

Besides generation of entanglement, e.g. MES, another transcendental task in quantum physics is the protection of this resource from the effects of decoherence and dissipation, which naturally destroy partially (for short times) and totally (for long times) the quantum correlations. Alternatively to the protection by the common methods as isolation, error correction [13–16], decoherence-free subspace [17, 18], etc., a kind of counteroffensive approach has been used lately, known in literature as quantum bath engineering (QBE) or engineered dissipation [19, 20], i.e. a procedure which permits driving an open quantum system to target states (correlated, coherent, etc.) by engineering the mechanisms of dissipation and decoherence. In this direction, during a relatively short period of time, many interesting theoretical and experimental studies proved that this strategy works well and can be very efficient for various physical systems [4, 20–31]. In this order of ideas, we present here a new example, applying efficiently the principle of QBE for the studied model, as will be explained in detail in the Section 3. In general lines, our proposal of QBE is based on a kind of nonlinear (two-mode) dissipation to the reservoir. Similar models [27–31] have been used recently.

In the present paper we investigate a theoretical model of a cavity network involving photonic Kerr non-linear effect, which provides the generation of MES in such a setup. Particularly, by a non-adiabatic evolution of the system from its ground state, possessing a very small fraction of entanglement, the preparation of MES is possible, as shown via the fidelity and negativity measures. We show that, the phenomenon of MES is conceivable under the conditions of closed and open system, e.g. considering the losses of the photons from the cavities. We also demonstrate how the MES could be protected in the open system, using a particular two-mode coupling to the environment, in such a way that it is possible to almost freeze the MES in the case of a phase flip noisy channel. Moreover, phenomenon of avoided level crossing (ALC) [32–34] appears in our model, and we study how this effect is related to the quantum correlations in the system, effect already discussed in the literature [16, 35–38]. Therefore, the main purpose of this work is to advance the field of quantum engineering, where original ideas for the production, control and protection of photonic MES are suggested and developed in a network of optical cavities under the approaches of closed and open system.

The remainder of this paper is structured in three sections.

In Sec. 2 we present a network model as a closed quantum system, defined in general for N cavities and numerically analyzed for the case of three cavities than could be, of course extended for more insight. We study the preparation of the MES and witness the entanglement through the Negativity and Fidelity. When the system evolves adiabatically, the phenomenon of avoided crossing is identified by the critical behavior of the bipartite and multipartite entanglement. These effects are illustrated and discussed.

In Section 3, the model of a cavity network is studied in the framework of an open quantum system, by considering two different damping mechanisms: (i) arbitrary photons of mode a and b leave the cavity at rates γ^a and γ^b , respectively; and (ii) the two-mode paired photons abandon the cavity at rate γ . Both damping processes occur under the condition of thermal environments at zero temperature. As a result, it is shown that by the damping of photons correlated in pairs, the MES decays slower in time, so concluding that such a bath engineering makes MES more robust. Moreover, if the decoherence to such environment corresponds to a phase flip noise channel, Eq.(21), then MES remains a steady state, evidencing its maximal fidelity. The last Section is devoted to the Conclusions.

II. THE CAVITY NETWORK MODEL WITHOUT LOSSES

We have an array of N two-mode cavities and inside of each one there is a non-linear medium which introduces a field-field interaction by Kerr self-phase modulation [39] and Kerr cross-phase modulation process [40]. Furthermore, photons can hop between nearest neighbor cavities. The total Hamiltonian (in units of \hbar) consists in three parts: a free part H_0 , a hopping term H_{hop} and photon-photon interaction term H_{int} .

$$H_0 = \sum_{i=1}^N [\omega_i^a a_i^\dagger a_i + \omega_i^b b_i^\dagger b_i] \quad (1)$$

$$H_{int} = \sum_{i=1}^N [k_a (\hat{n}_i^a)^2 + k_b (\hat{n}_i^b)^2 + k_{int} \hat{n}_i^a \hat{n}_i^b] \quad (2)$$

$$H_{hop} = \sum_{i=1}^{N-1} J_i [a_i^\dagger a_{i+1} e^{i\phi_a} + b_i^\dagger b_{i+1} e^{i\phi_b} + h.c.] \quad (3)$$

Notice that the interaction Hamiltonian (2) [41, 42], indicating the contribution of the Kerr medium, involves only quadratic elements. The first two terms correspond to the self-phase modulation process, and usually appear as $(a^\dagger)^2(a)^2$, but this product of the creation and annihilation operators can be reordered using the commutation relationship to get Eq.(2), which yields constants and linear terms which can be neglected since they commute with the Hamiltonian. The third term is related to the Kerr cross-phase modulation, and introduces an effective interaction between the two modes. In order to simplify the problem, we can eliminate H_0 going to the interaction picture with the unitary transformation $U = e^{-iH_0 t}$, which leaves H_{int} and H_{hop} invariant under the conditions $\omega_i^a = \omega^a$ and $\omega_i^b = \omega^b$. For the rest of the paper, our Hamiltonian will have two parts only, H_{hop} and H_{int} .

A. Preparation of Maximally Entangled State (MES)

The first objective of this study, is to prepare MES from an arbitrary disentangled or partially entangled state by applying the above Hamiltonian in the proposed photonic network. Such a MES have been extensively studied [1], and the general form of these states can be expressed by

$$|MES\rangle = \sum_{\vec{n}} \lambda_{\vec{n}} |n_1, \dots, n_N\rangle_a \otimes |n_1, \dots, n_N\rangle_b, \quad (4)$$

where $|n_1, n_2, \dots, n_N\rangle_{a(b)}$ represents the state with n_i photons in cavity i for the mode $a(b)$, while \vec{n} runs over all possible combinations of $\{n_1, \dots, n_N\}$. It is important to notice that there are the same number of photons for each mode in each cavity. Next, we apply the Hopping Hamiltonian to this state:

$$\begin{aligned}
H_{hop}|MES\rangle &= \sum_{i=1}^{N-1} \sum_{\vec{n}} J_i \lambda_{\vec{n}} [e^{i\phi_a} \sqrt{n_i+1} \sqrt{n_{i+1}} |n_1, \dots, n_i+1, n_{i+1}-1, \dots, n_N\rangle_a \otimes |n_1, \dots, n_N\rangle_b \\
&+ e^{-i\phi_a} \sqrt{n_i} \sqrt{n_{i+1}+1} |n_1, \dots, n_i-1, n_{i+1}+1, \dots, n_N\rangle_a \otimes |n_1, \dots, n_N\rangle_b \\
&+ e^{i\phi_b} \sqrt{n_i+1} \sqrt{n_{i+1}} |n_1, \dots, n_N\rangle_a \otimes |n_1, \dots, n_i+1, n_{i+1}-1, \dots, n_N\rangle_b \\
&+ e^{-i\phi_b} \sqrt{n_i} \sqrt{n_{i+1}+1} |n_1, \dots, n_N\rangle_a \otimes |n_1, \dots, n_i-1, n_{i+1}+1, \dots, n_N\rangle_b]. \tag{5}
\end{aligned}$$

Now, by replacing the indices $(n_i+1) \rightarrow n_i$ and $(n_{i+1}-1) \rightarrow n_{i+1}$, in the third term, and for the fourth term, $(n_i-1) \rightarrow n_i$ and $(n_{i+1}+1) \rightarrow n_{i+1}$, we readily get,

$$\begin{aligned}
H_{hop}|MES\rangle &= \sum_{i=1}^{N-1} J_i \sum_{\vec{n}} [\lambda_{\vec{n}} e^{i\phi_a} \sqrt{n_i+1} \sqrt{n_{i+1}} |n_1, \dots, n_i+1, n_{i+1}-1, \dots, n_N\rangle_a \otimes |n_1, \dots, n_N\rangle_b \\
&+ \lambda_{\vec{n}} e^{-i\phi_a} \sqrt{n_i} \sqrt{n_{i+1}+1} |n_1, \dots, n_i-1, n_{i+1}+1, \dots, n_N\rangle_a \otimes |n_1, \dots, n_N\rangle_b \\
&+ \lambda_{\{n_i-1, n_{i+1}+1\}} e^{i\phi_b} \sqrt{n_i} \sqrt{n_{i+1}+1} |n_1, \dots, n_i-1, n_{i+1}+1, \dots, n_N\rangle_a \otimes |n_1, \dots, n_N\rangle_b \\
&+ \lambda_{\{n_i+1, n_{i+1}-1\}} e^{-i\phi_b} \sqrt{n_i+1} \sqrt{n_{i+1}} |n_1, \dots, n_i+1, n_{i+1}-1, \dots, n_N\rangle_a \otimes |n_1, \dots, n_N\rangle_b]. \tag{6}
\end{aligned}$$

We can regroup Eq.(6) and take $J = J_i$ such that

$$\begin{aligned}
H_{hop}|MES\rangle &= J \sum_{i=1}^{N-1} \sum_{\vec{n}} [(\lambda_{\vec{n}} e^{i\phi_a} + \lambda_{\{n_i+1, n_{i+1}-1\}} e^{-i\phi_b}) \\
&\times \sqrt{n_i+1} \sqrt{n_{i+1}} |n_1, \dots, n_i+1, n_{i+1}-1, \dots, n_N\rangle_a \otimes |n_1, \dots, n_N\rangle_b \\
&+ (\lambda_{\vec{n}} e^{-i\phi_a} + \lambda_{\{n_i-1, n_{i+1}+1\}} e^{i\phi_b}) \\
&\times \sqrt{n_i} \sqrt{n_{i+1}+1} |n_1, \dots, n_i-1, n_{i+1}+1, \dots, n_N\rangle_a \otimes |n_1, \dots, n_N\rangle_b]. \tag{7}
\end{aligned}$$

One can see that it is possible to have zero hopping energy, by generating vanishing prefactors in Eq.(7). Then, using this idea we get the following condition for the first prefactor,

$$\lambda_{\vec{n}} e^{i(\phi_a + \phi_b + \pi)} = \lambda_{\{n_i+1, n_{i+1}-1\}}. \tag{8}$$

The previous condition indicates that a single hopping is equivalent to introducing a phase $e^{i(\phi_a + \phi_b + \pi)}$. Since the system is periodic, we can repeat this process N times to get,

$$\lambda_{\vec{n}} e^{iN(\phi_a + \phi_b + \pi)} = \lambda_{\vec{n}}, \tag{9}$$

and with the above result, the condition for having vanishing hopping energy is,

$$(\phi_a + \phi_b) = \frac{(2m - N)\pi}{N}, \tag{10}$$

with m an integer number. The same condition for the phases applies to the other term in Eq.(7). This result is very important, summarizing the first step towards the generation of a MES. The second step, is to generate a zero interaction energy, then we apply the H_{int} to the MES state,

$$H_{int}|MES\rangle = \sum_{\vec{n}} \sum_{i=1}^N \lambda_{\vec{n}} (k_a + k_b + k_{int}) n_i^2 |n_1, \dots, n_N\rangle_a \otimes |n_1, \dots, n_N\rangle_b. \tag{11}$$

It is worth noticing that the terms inside the parenthesis do not depend on n_i because of the form of the MES state, where there is the same number of photons in each mode. Following the approach in [42], the authors showed

that $k_{int} = 2\sqrt{k_a k_b}$. The factor $k_{a(b)}$ is proportional to the real part of the third-order susceptibility, $\chi^{(3)}$, which can be negative [43, 44]. Thus, setting $k_a = k_b = -k$, we get zero eigenvalue for both the Interaction and full Hamiltonian.

Finally, replacing condition (8) in Eq.(4) we get the MES definition,

$$|MES\rangle = \sum_{\vec{n}} \frac{1}{\sqrt{d}} e^{i\frac{2\pi m}{N} p_{\{n_1, \dots, n_N\}}} |n_1, \dots, n_N\rangle_a \otimes |n_1, \dots, n_N\rangle_b, \quad (12)$$

where $p_{\{\dots, n_j+1, n_{j+1}-1, \dots\}} = p_{\{\dots, n_j, n_{j+1}, \dots\}} + 1$ and d is the dimension of the Hilbert space [45].

One can reach the MES dynamically by varying the phase non adiabatically, as depicted in Fig.1 by the red triangles, where we set $\phi_a = \phi_b = \phi$. When $m = 3$ and $\phi = \pi/2$ the MES state that we reached is:

$$\begin{aligned} |MES\rangle = & \frac{1}{\sqrt{6}} (|011\rangle \otimes |011\rangle + |101\rangle \otimes |101\rangle + |110\rangle \otimes |110\rangle \\ & + |200\rangle \otimes |200\rangle + |020\rangle \otimes |020\rangle + |002\rangle \otimes |002\rangle). \end{aligned} \quad (13)$$

On the other hand, if the phase varies adiabatically, then the system follows its initial eigenstate, patterned by the blue squares. The effects of the avoided level crossing will be discussed in the subsection C.

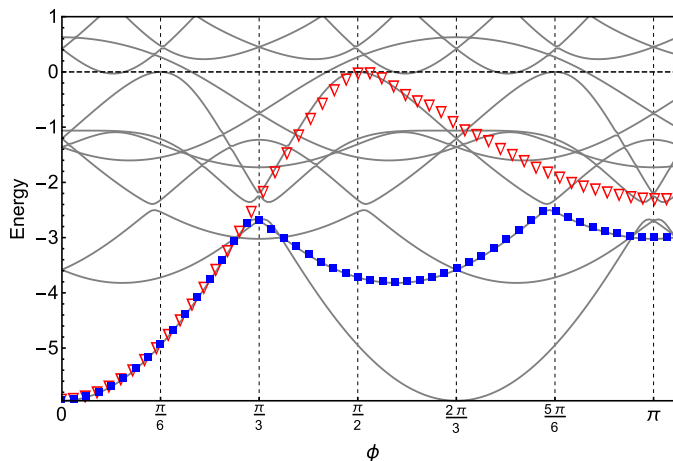


FIG. 1: Energy levels as function of the phase. Preparation of MES by non adiabatic variation of phase (red triangles); ground state evolution in the adiabatic passage (blue squares). Here $k_a = k_b = J$.

B. MES: bipartite or multipartite correlations?

We consider our present system composed of six qutrits (states with 0,1 and 2 photons) defined by three cavities and two modes per cavity. The quantum correlations in a system of any dimension, i.e. qudits, are usually measured by the Negativity [46, 47]. In our particular case, in order to quantify the amount of bipartite (two-body) quantum correlation, we trace over four of the qutrits and use Negativity to calculate the correlations between the residuary qutrits.

In general, for subsystems X and Y and an associated density matrix ρ_{XY} , the Negativity is defined as

$$\mathcal{N}(\rho_{XY}) = \sum_i \frac{|\lambda_i| - \lambda_i}{2}, \quad (14)$$

where λ_i are the eigenvalues of the partial transpose of the density matrix, $\rho^{T_{X(Y)}}$, with respect to one of the subsystems. It essentially measures the degree to which $\rho^{T_{X(Y)}}$ fails to be positive, and therefore it can be considered as a quantitative version of Peres's criterion for separability [48].

After preparing the target MES, it is important to evaluate the degree of entanglement of this state. The MES defined by Eq.(13) is mostly a global (multipartite) entangled state between two different modes localized in three

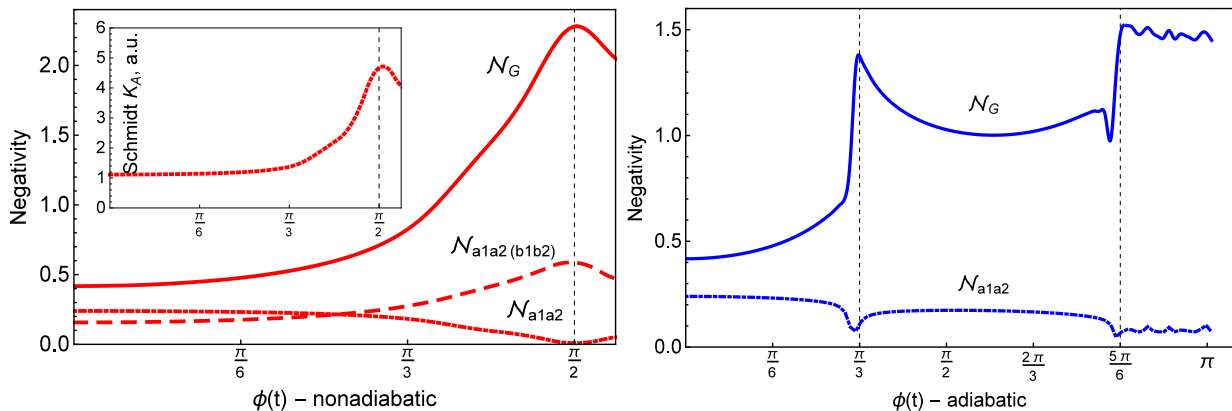


FIG. 2: (left) Global (\mathcal{N}_G) and partial ($\mathcal{N}_{a1a2(b1b2)}$) multipartite Negativity reach a maximum when approaching the MES phase ($\pi/2$), while bipartite correlations (\mathcal{N}_{a1a2}) vanish. Inset: evolution of \mathcal{N}_G and Schmidt number agrees. (right) Two avoided level crossing are witnessed by an abrupt increment of \mathcal{N}_G , while decreasing bipartite correlations, \mathcal{N}_{a1a2} . The parameters are as in Fig.1.

cavities. This means that all possible bipartite correlations, say mode a and b of the same cavity or different cavities have no entanglement (zero Negativity). Negativity is only a sufficient condition for entanglement, however, by tracing out over four of the qutrits, ending with only two qutrits, one can realize that the final state has no quantum correlation between its parts. Even more, the MES has no correlation between subsystems of the same mode, not bipartite correlation (\mathcal{N}_{a1a2}), as shown by dot-dashed curve in Fig. 2a, nor tripartite correlation (π_{a1a2a3}) plotted in Fig. 3 and shown by bullets. Nevertheless, we cannot say that the MES state belongs to the *GHZ* class of multipartite entangled states. We recall that for the GHZ state, when eliminating one of the qudits, all correlations are destroyed, ending with a state proportional to the identity matrix. In our case, if we trace out over only one cavity, for example cavity three, we still find correlations between the remaining modes, evidenced when calculating $\mathcal{N}_{a1a2(b1b2)}$ similar to Eq.(17) and represented with a dashed curve in Fig. 2a.

Because of the high dimension of the system, to calculate any global multipartite measure of correlations, considering both modes is a difficult task.

For example, in order to measure tripartite correlations for the same mode, we used two different definitions found in literature, as in [49]

$$\pi_{a1a2a3} = \frac{1}{3} \sum_{i=1}^3 \pi_{ai}, \quad (15)$$

with $\pi_{a1} = \mathcal{N}_{a1(a2a3)}^2 - \mathcal{N}_{a1a2}^2 - \mathcal{N}_{a1a3}^2$; and as in [50]

$$\mathcal{M}_{a1a2a3} = \sqrt[3]{\mathcal{N}_{a1(a2a3)}\mathcal{N}_{a2(a1a3)}\mathcal{N}_{a3(a1a2)}}. \quad (16)$$

In the next section (see Fig. 4), we compare both measures during the preparation of the MES state.

For a more general situation, in order to investigate the multipartite correlations, we consider an approximate calculation, which can be carried out in a relatively simple way, by considering the symmetry properties in our model. For example, we may assume that for each mode one has an averaged state for the three cavities which are identical, so instead of considering three qutrits, there will be one qudit of dimension $d = 3^3$. Applying the same idea for the other mode, we end up with two qudits, for which may calculate the standard negativity measure as in Eq.(14), as follows

$$\mathcal{N}_G = \mathcal{N}_{a1a2a3(b1b2b3)}, \quad (17)$$

where the partial transpose is taken on mode b in the three cavities. Using this approach, we get a value that gives us a qualitative estimation of the the global correlation between the two modes, considering that for the MES, the bipartite and tripartite correlations vanish.

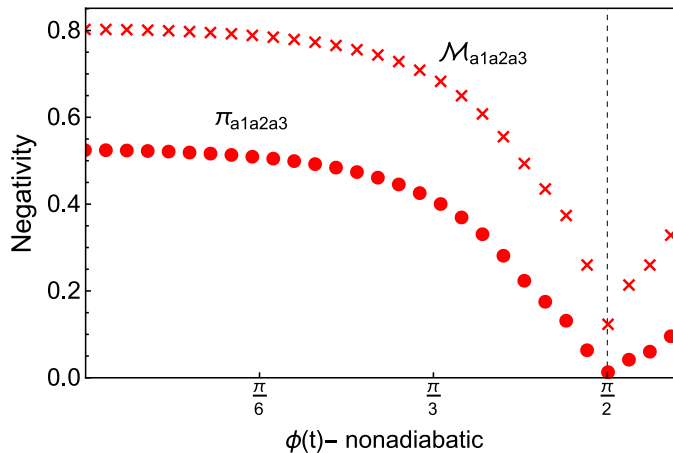


FIG. 3: Evolution of Negativity measuring the tripartite correlations using Eq.(15) (circles) and Eq.(16) (crosses) for the nonadiabatical passage for the same parameters as in Fig.2.

C. Negativity witnessing MES and avoided level crossing

In this subsection we analyze the quantum correlations measured by the Negativity, and for verification the Schmidt number was computed as well. As was explained above, to engineer the MES during the dynamics of the system one should satisfy two conditions: (i) $k_a + k_b + k_{int} = 0$ resulting from Eq.(11), and (ii) managing the total phase given by Eq.(10). The first condition can be achieved as in references [42–44], and in our calculations one just fixes $k_a = k_b = -k_{int}/2$. In order to fulfill dynamically the second condition, one could vary the phase both adiabatically and non-adiabatically to meet the target value.

Let's start by managing the non adiabatic variation of the phase, so initiating in the ground state, the system follows the track as represented in Fig. 1 by the red triangles. We see that for the phase equal to $\pi/2$ the system evolves to the state with zero energy, which could be the MES. In order to check this, we compute the value of entanglement as shown in Fig. 2a. In the main plot we show three curves, where the continuous line represents the global (multipartite) entanglement between the modes a and b in three cavities, the dashed line depicts the entanglement between the modes a and b in two cavities ($\mathcal{N}_{a1a2(b1b2)}$), i.e. the partial multipartite correlation, and finally the dot-dashed curve evidences the bipartite entanglement of the mode a for two different cavities. The results are quite clear. We find that the maximal value of the multipartite entanglement measured by the Negativity as well the Schmidt number (inset of Fig. 2a) occur in the region where the phase is $\pi/2$, so witnessing the MES as given in Eq.(13). On the other hand, the minimal value of the bipartite entanglement indicates that the MES has genuinely multipartite correlations, distributed between the modes a and b , additionally evidenced by the partially multipartite entanglement as shows the dashed curve. We also computed the Negativity, not shown here, for the bipartite states of modes a and b in the same or different cavities, but the results show that the entanglement is zero at all times. For a deeper insight on the correlations, we computed the tripartite correlations for the mode a and represent numerically the comparison between the two different methods as shown in Fig. 3, where we see that the tripartite entanglement computed by Eq.(15) becomes zero in $\pi/2$ indicating once more that the MES has multipartite correlations between the modes, hence one can conclude that the method proposed in [49] is more appropriate, at least for our system.

Next, we continue by studying the adiabatic variation of the phase, as is represented in the Fig. 1 by the blue squares path. We readily notice that the system follows its ground state during all the evolution and never reach a MES. However, we observe another effect occurring during the dynamics of the eigenstate, the so-called avoided level crossing (ALC). The ALC is a region where two or more energy levels of the system are close enough such that the dynamics might follow one path with almost no change in the wave function or jump to a fairly different state (that occurs in the case of non adiabatic variation of phase). The selection of one path or the other can be tuned by changing one parameter, which increases (decreases) the speed at which the wave function undergoes to the avoided crossing leading to the non adiabatic (adiabatic) passage, see Fig. 1. It is noted that when approaching the ALC, the evolution of the state turns out to be very complex leading some times to chaos [32, 36, 51] or quantum phase transitions [52]. The signature of an ALC is not always easy to establish by just looking at the time evolution of the wave function. Quantum correlations (QC) play an important role in detecting the criticality [53–55]. It has been shown that for different systems, the QC change considerably in this region, and these may reach an extremal value [35–38, 54]. For multiparticle systems, the real witness is the multipartite rather than bipartite correlation.

Furthermore, it has been pointed out for a spin chain that at an ALC, the multipartite correlation increases while the bipartite correlation decreases [36]. This behavior indicates that in this region a collective effect shows up (global correlation), rather than a nearest-neighbor dynamics (two-body interaction).

In order to establish with more certainty the effect of ALC in our model, we analyzed the dynamics of the entanglement measured by Negativity. In Fig. 1 we find that ALC seems to occur in the regions of $\phi \approx \pi/3$ and $\phi \approx 5\pi/6$. The evolution of the Negativity as seen in Fig. 2b, shows clearly the position of the ALC and is perfectly witnessed by an abrupt change in the dynamics, evidencing maximal values for multipartite entanglement and minimal values for bipartite entanglement. It should be mentioned that the Schmidt number has very similar behavior. Our results are in good agreement to a similar effect observed in [35] and confirm the more general conclusions given in [36], hence shedding more light on the importance of QC in witnessing phenomena like ALC, etc.

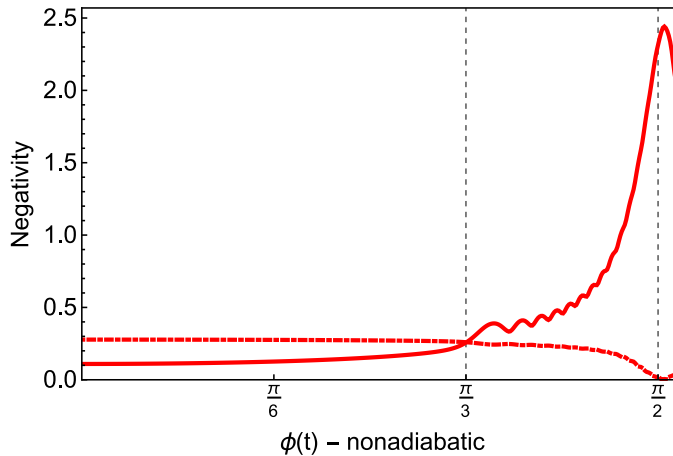


FIG. 4: Global entanglement (solid line) and bipartite entanglement (dot-dashed line) similar as in Fig. 2a, except that $k_a = k_b = J/4$.

To conclude this section, we find and emphasize here the importance of the adiabatic and non adiabatic passages in our model. Even if the adiabatic path that does not lead to a considerable change in the energy, there is a sudden transition in the evolution of interspecies multipartite entanglement (modes a and b in whole network) and inter-site bipartite entanglement (same mode in two different cavities), effect shown in Fig. 2b, which is similar to the one described by Karthik *et al.* [36]. In the nonadiabatic passage leading to the MES, one would also expect to observe a particular behavior of the Negativity which changes spontaneously its value in the region of ALC or *exceptional point*, as named sometimes in literature [32–34]. This effect is not observed well in Fig. 2a but is better visible for the smaller gaps between the levels at the ALC, which could be managed, e.g. by decreasing the rate k/J in Eq.(2) (see Fig. 4, where a more abrupt increase of the global entanglement is shown from the ALC region on, as the path reaches the MES in its dynamics).

III. DAMPING EFFECTS IN THE PHOTONIC NETWORK

A. Preparation of a MES with losses

In Fig. 1 we showed that the MES (13) can be prepared from the ground state by changing the phase, which as a function of time can be explicitly written as $\phi = \alpha t$. Notice that α will give the speed of the system. When α is small enough, the system will follow the adiabatic path, otherwise it will follow the non adiabatic path. However, not all the non adiabatic paths will lead to the MES, actually, there is a small range of values of α (α_{opt}) that optimize the MES preparation, reaching a high Fidelity ($\mathcal{F} = \text{tr}[\rho|MES\rangle\langle MES|]$) [56]. We found that for $k = J/16$ and $\alpha_{opt} = 3 * 10^{-4} J$ the Fidelity is $\mathcal{F} \approx 0.98$. The nonlinear interaction k is related to the height of the gap at the avoided crossing. If this gap is considerably diminished such that even for a slow tuning of the phase, *i.e.* small α , the system still goes through the non adiabatic path, then the probability of reaching the MES is very high. That is why we decreased k down to $J/16$. Unfortunately, α_{opt} depends on different parameters, as k , J and γ if losses were considered. Then, by decreasing k we have to decrease α too, in order to find α_{opt} . For the case where the interaction with the environment is not negligible, this mechanism is not effective, since we need to vary the phase very slowly, and eventually losses will lead the state to a different path before becoming a MES. In the presence of

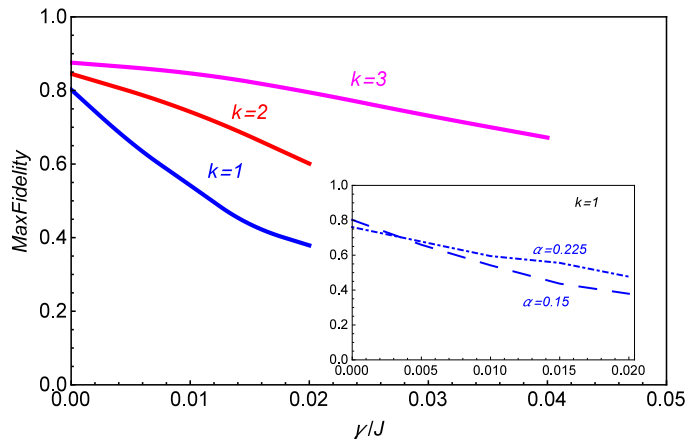


FIG. 5: The losses rate γ deteriorates the preparation of the MES, but this can be overcome by increasing the nonlinear interaction k . Inset: Another approach to deal with losses is to increase the speed α , which for higher losses increases the Fidelity.

losses, it would be convenient for the system to quickly reach the phase $\pi/2$. Another approach is to increase k with respect to J . In this case, as we decrease the hopping strength the inter-site correlation becomes smaller, while the inter-species interaction gets stronger. Under this condition the energy spectrum shrinks down, and the ground state (from which we start in the dynamics leading the MES) becomes very close to the zero energy level, thus closer to the MES. This means that for large α , which implies going faster to the MES, one still gets a good Fidelity ($\mathcal{F} \approx 0.9$) while at the same time losses are reduced. Another way to understand this, is by comparing the hopping Eq.(3) and the interaction Eq.(2) Hamiltonians. When k gets bigger the interaction term dominates over the hopping. Because of this, the dependence with α , which appears in the condition (7), is not that relevant, since the condition (11) dominates and it is independent of α .

In order to simulate losses, we assume that each mode interacts with its own reservoir at zero temperature, making the photons jump out of the cavities. We use the master equation (ME) approach [57]. The equation of motion for the density operator is given by,

$$\dot{\rho} = -i[H, \rho] + \mathcal{L}_a(\rho) + \mathcal{L}_b(\rho), \quad (18)$$

where

$$\mathcal{L}_\Lambda = \sum_{k=1}^3 \frac{\gamma_k^\Lambda}{2} (2\Lambda_k \rho \Lambda_k^\dagger - \{\Lambda_k^\dagger \Lambda_k, \rho\}), \quad (19)$$

with the operator $\Lambda = \{a, b\}$, $k = \{1, 2, 3\}$ representing different cavities, and $\gamma^a(\gamma^b)$ the decay rate for mode $a(b)$.

In Fig. 5 we show the variation of the maximum of the Fidelity with respect to the MES as a function of the losses rate (γ). As one would expect, as we increase the loss rate, the maximum Fidelity decreases. However, in the main plot we see that by increasing the nonlinear interaction k , holding γ fixed, we manage to generate the MES with higher Fidelity. Notice that each curve is plotted for its corresponding α_{opt} at $\gamma = 0$. As we said above, α_{opt} is a function of γ , but we will discuss this case later on. We found numerically that there is a critical rate (γ_c), above which the Fidelity only decreases, *i.e.*, there is no global maximum for the Fidelity at $\pi/2$, evidencing that the system will not get closer to the MES with the given set of parameters. For example, for $\alpha = 0.15J$ and $k = J$ we found that $\gamma_c \approx 0.02J$. This means that if in the system losses cannot be controlled to be below this threshold, the only way to get the MES is by tuning the other parameters.

Let's now discuss the dependence of α_{opt} with γ . By holding k constant, as losses increase one can increase the speed α to obtain higher Fidelity. As we explain above, the reason why this happens is that the system will get faster to the phase $\pi/2$, which means going to the MES before losses take it through a different path. However, this behavior is not well evidenced for large k ($k \geq 3$), since the system becomes insensitive to the variation of α . Then, the consideration of the dependence $\alpha_{opt}(\gamma)$ is better observed for smaller k . In the Inset of Fig. 5, we compare the maximum of the Fidelity as a function of γ for $\alpha = 0.15$ (bottom curve of the main plot) and $\alpha = 0.225$. We chose for this plot $k = J$. We see that because of $\alpha = 0.15$ (dashed line) is the optimal value at $\gamma = 0$, this curve starts above $\alpha = 0.225$ (dot-dashed line). Nevertheless, when increasing the losses both curves intercept and beyond that $\alpha = 0.225$ becomes the new optimal value. This method works as a mechanism for dealing with losses.

B. Robustness against noise

In this subsection, we are interested in preserving the MES (13). In order to counteract the effects of the environment, at least for a short time of the evolution, a quantum error correction protocol [13] could be implemented. However, this is not a feasible solution, since it will require the encoding of a very large state [14], which is not practical. A Decoherence-Free Subspace (DFS) [17, 18] does not lead to any significant result either, since a common reservoir for the whole system, as well as an enlargement of the system would be needed. An interesting approach to protect the MES against decoherence could rely on reservoir engineering. Let's assume that each cavity interacts with its own reservoir, but the two modes inside a cavity will interact in a certain way such that if one experiences a jump, the other mode will follow the first one, similar as in [30]. However, the non-linear losses not appear naturally in the standard optical cavities/resonators and should be artificially stimulated in order to compete with the single photon damping, usual for such devices. Experimentally, such non-linear damping is not an easy task, nevertheless an intuitive experiment could be considered were the damping occurs in an absorbing medium resonant with two-photon transitions, e.g. for our model. More complex experiment was proposed very recently [27], were the authors realize two-photon dissipation at the rate of the same order of magnitude as the single-photon decay rate (i.e. γ is approximately similar in Eqs. (19) and (20)). Even more, the authors conclude: "The ratio between these two rates can be further improved within the present technology by using an oscillator with a higher quality factor and increasing the oscillator's nonlinear coupling to the bath" (page 857, last paragraph).

Under this two photon approximation, the corresponding Lindblad term of ME can be rewritten as

$$\mathcal{L}_\Sigma = \sum_{k=1}^3 \frac{\gamma^k}{2} (2\Sigma_k \rho \Sigma_k^\dagger - \{\Sigma_k^\dagger \Sigma_k, \rho\}), \quad (20)$$

where $\gamma^a = \gamma^b = \gamma$ and we introduced a new collective operator $\Sigma = ab$. Notice that operator Σ includes modes a and b for the same cavity. Nevertheless, it is easy to see that this approximation for the interaction with the reservoir it is not equivalent to have the two modes in a common reservoir, in which case the correct substitution would be $\Sigma = a + b$. In Fig.6 we compare this new way of modeling the reservoir (20) to the noise channel defined by Eq.(19) by measuring the Fidelity with respect to the MES. Notice that the MES is more robust against the decoherence for the *coupled decay* type of reservoir, i.e. provided that both modes inside each cavity decay cooperatively.

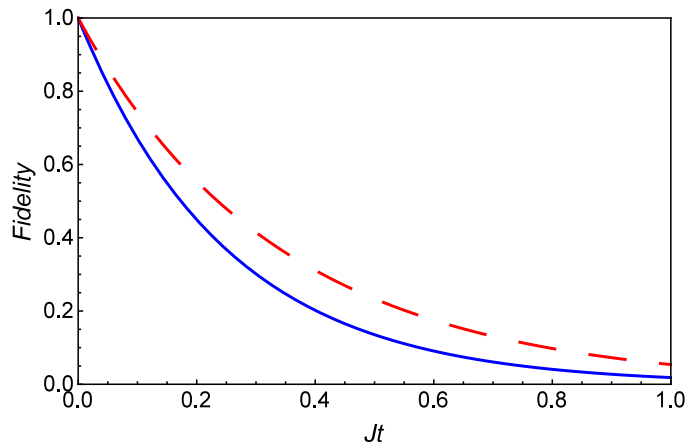


FIG. 6: The time evolution of Fidelity with respect to the MES in case of different noise channels. Fidelity for the case of engineered reservoir (red dashed), given by Eq.(20), decays slower as compared to the case of standard reservoir (blue line), described by Eq.(19). Here $\gamma = J$, $k_a = k_b = J/2$.

Nevertheless, dissipation may not be the only source of noise, in fact, a Phase Flip (PF) mechanism [13] will lead to a strong decoherence. It is noticed that the MES state (13), is very sensitive to decoherence (losses of the off diagonal elements). Then, the PF mechanism, which because of its definition leaves the diagonal elements invariant and only changes the off diagonal elements, could reproduce for example, the decrease in the Fidelity with respect to the MES state. Going in this direction, we propose a PF noise channel, by replacing the creation and annihilation operators in Eq.(19) by,

$$\sigma_\alpha = |0\rangle\langle 0| + e^{i\theta}|1\rangle\langle 1| + e^{i\theta}|2\rangle\langle 2|, \quad (21)$$

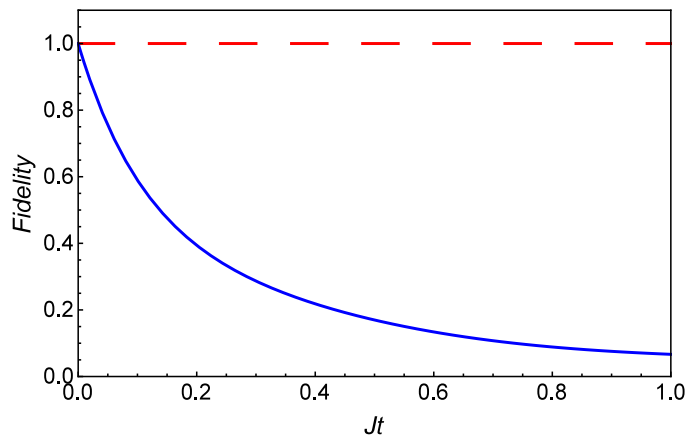


FIG. 7: As result of the symmetry between the different modes composing the MES, we observe numerically and analytically, that this state remains unaltered (red dashed line) under a Phase Flip noise channel that interacts with the system by Eq.(20). For an interaction of the type Eq.(19) the fidelity decays as should be expected. $\gamma = J$, $k_a = k_b = J$.

with $\theta = \pi$. This operator introduces a phase on the state if there is at least one photon in the mode, otherwise it leaves the state invariant. It would be interesting now to see how this PF noise acts on the MES by combining it with the two damping mechanisms defined by Eqs. (19) and (20). This is shown in Fig. 7. For the case of the coupled decay (20) we have to replace operator Σ by $P = \sigma_a \sigma_b$. We observe in Fig. 7 that under the coupled decay approximation for the noise channel (20), the MES state is completely robust against the Phase Flip noise channel. On the contrary, for the case of the noise channel described in (19) the fidelity decays rapidly.

IV. CONCLUSION

Entanglement is a fundamental tool for quantum information tasks, however, and unfortunately, it is very fragile with respect to environmental noise which poses a problem of not only creating entanglement, but a practical way of protecting it. In this work, we addressed the problem of generation and protection of a MES in an optical network. We showed that one can generate a MES as a zero energy eigenstate of the Hamiltonian of the system, that satisfies the conditions (7) and (11). We also discuss the dynamics to reach such a state, starting from the ground state of the system. If we vary the phase in time, with a velocity α , it takes a rapid evolution (non adiabatic) to jump over the avoided crossing gap to reach the desired state. On the other hand, for a slow time evolution (small α), the system will follow the same original state. In this case, we observe that when approaching the gap region, the global entanglement experiences a maximum while the bi and three partite entanglements show a minimum, providing the evidence that a collective phenomena takes place. Also, we suggest, via reservoir engineering, how to protect the MES from decoherence. In particular, we show that for a collective decay model, i.e. Eq. (20), the system is robust under decoherence mechanisms such as phase flip. Finally, let's discuss the experimental realization of our proposal. We focus first on the hopping term in Eq. (3). The coupling between the cavities can be achieved mainly in two different ways [58], either via an optical fiber [59] or by tunnel effect [60]. The hopping we modeled is a general expression that fits well with others model like Bose-Hubbard model [60] and super conducting qubits [61], and it can be tuned to be of the order of MHz. We choose to scale all the parameter with the hopping strength (J), such that some conclusion of this work can be extended to others system. Then, in order to see the feasibility of the experiment, we are only interested in the rate k/J , with k representing the nonlinearities. The Kerr self interaction naturally appears in some media as a result of a non-zero third-order electric susceptibility, but its effect is negligible on the level of few photons. However, the strong interaction of the light mode with atoms inside a cavity QED, under particular circumstances, mediates strong nonlinear interaction among the photons of the cavity mode [62]. The Kerr cross interaction can be more difficult to realize for photons, but as self interaction it should be done effectively through a nonlinear medium, e.g., atoms. Furthermore, in the polaritonic basis, both Kerr interactions appears for the case of four level atoms [63], indicating that this approach is possible. Once again, in Bose Hubbard model these nonlinear interactions appears naturally [45]. For a three level atom configuration, the nonlinear interaction can be explained by the Stark shift [60], and this shift have been measured experimentally [64] to be of the order of MHz. Even more, in recent experiments for super conducting qubits, similar nonlinear strength has been found, for self and cross interaction [26]. To conclude, the rates we used in our simulations can be obtained experimentally in a variety of systems.

V. ACKNOWLEDGMENT

The authors would like to thank the support of projects Fondecyt No. 1140994 and Conicyt-PIA anillo ACT-1112 “Red de análisis estocástico y aplicaciones”. One of us (R.C.) also thanks the support of Fondecyt (postdoctoral fellowship No. 3160154).

-
- [1] R. Horodecki, P. Horodecki, M. Horodecki, K. Horodecki, *Rev. Mod. Phys.* **81**, 865 (2008).
 - [2] V. Vedral, *Nat. Phys.* **10**, 256 (2014).
 - [3] M.-J. Zhao, *Phys. Rev. A* **91**, 012310 (2015).
 - [4] M. J. Kastoryano, F. Reiter and A. S. Sørensen, *Phys. Rev. Lett.* **106**, 090502 (2011).
 - [5] A. Datta, A. Shaji and C.M. Caves, *Phys.Rev.Lett* **100**, 050502 (2008).
 - [6] M. Piani, P. Horodecki, R. Horodecki, *Phys. Rev. Lett.* **100**, 090502 (2008).
 - [7] J.-S. Xu, *et al.*, *Nature Commun.* **1**, 7 (2010); J.-S. Xu, *et al.*, *Nature Commun.* **4**, 2851 (2013).
 - [8] M. Piani, S. Gharibian, G. Adesso, J. Calsamiglia, P. Horodecki, and A. Winter, *Phys. Rev. Lett.* **106**, 220403 (2011).
 - [9] A. Streltsov, H. Kampermann, and D. Bruß, *Phys. Rev. Lett.* **106**, 160401 (2011).
 - [10] G. Adesso, V. D'Ambrosio, E. Nagali, M. Piani, F. Sciarrino, *Phys. Rev. Lett.* **112**, 140501 (2014).
 - [11] B. P. Lanyon, P. Jurcevic, C. Hempel, M. Gessner, V. Vedral, R. Blatt, and C. F. Roos, *Phys. Rev. Lett.* **111**, 100504 (2013).
 - [12] A. Orioux, M.A. Ciampini, P. Mataloni, D. Bruß, M. Rossi, and C. Macchiavello, *Phys. Rev. Lett.* **115**, 160503 (2015).
 - [13] M. A. Nielsen and I. L. Chuang, *Quantum Computation and Quantum Information* (Cambridge University Press, Cambridge, 2010).
 - [14] B. Zeng, D. L. Zhou, Z. Xu, C. P. Sun and L. You, *Phys. Rev. A* **71**, 022309 (2005).
 - [15] M. H. Devoret and R. J. Schoelkopf, *Science* **339**, 1169 (2013).
 - [16] M. D. Reed, in *Entanglement and Quantum Error Correction with Superconducting Qubits*, Ph.D. thesis, Yale University (2013).
 - [17] D. A. Lidar, I. L. Chuang and K. B. Whaley, *Phys. Rev. Lett.* **81**, 2594 (1998).
 - [18] D. Mundarain and M. Orszag, *Phys. Rev. A* **75**, 040303(R) (2007).
 - [19] J. F. Poyatos, J. I. Cirac, and P. Zoller, *Phys. Rev. Lett.* **77**, 4728 (1996).
 - [20] F. Verstraete, M.M. Wolf, and J. I. Cirac, *Nat. Phys.*, **5**, 633 (2009).
 - [21] J. T. Barreiro, *et al.*, *Nature Physics* **6**, 943 (2010).
 - [22] H. Krauter, C. A. Muschik, K. Jensen, W. Wasilewski, J. M. Petersen, J. I. Cirac, and E. S. Polzik, *Phys. Rev. Lett.* **107**, 080503 (2011).
 - [23] K. W. Murch, *et al.*, *Phys. Rev. Lett.* **109**, 183602 (2012).
 - [24] G. Kordas, S. Wimberger, and D. Witthaut, *Europhys. Lett.* **100**, 30007 (2012).
 - [25] C. Aron, M. Kulkarni, and H. E. Türeci, *Phys. Rev. A* **90**, 062305 (2014).
 - [26] E. T. Holland, *et al.*, *Phys. Rev. Lett.* **115**, 180501 (2015).
 - [27] Z. Leghtas, *et al.*, *Science* **347**, 6224 (2015).
 - [28] A. Mikhalychev, D. Mogilevtsev and S. Kilin, *J. Phys. A: Math. Theor.* **44** 325307 (2011).
 - [29] D. Mogilevtsev, A. Mikhalychev, V. S. Shchesnovich, and N. Korolkova, *Phys. Rev. A* **87**, 063847 (2013).
 - [30] K.V.S. Shiv Chaitanyaa, S. Ghoshb and V. Srinivasan, *J. Mod. Opt.* **61**, 1409 (2014).
 - [31] R. Azouit, A. Sarlette, P. Rouchon, arXiv:1503.06324 and arXiv:1511.03898
 - [32] W. D. Heiss and A. L. Sannino, *J. Phys. A: Math. Gen.* **23**, 1167 (1990).
 - [33] M. Bhattacharya and C. Raman, *Phys. Rev. Lett.* **97**, 140405 (2006); *ibid*, *Phys. Rev. A* **75**, 033405 (2007).
 - [34] H. Eleuch and I. Rotter, *Fortschr. Phys.* **61**, 194 (2013).
 - [35] R. Gonzalez-Ferez and J. S. Dehesa, *Phys. Rev. Lett.* **91**, 113001 (2003).
 - [36] J. Karthik, A. Sharma, and A.Lakshminarayan, *Phys. Rev. A* **75**, 022304 (2007).
 - [37] S. Oh, Z. Huang, U.Peskin, and S. Kais, *Phys. Rev. A* **78**, 062106 (2008).
 - [38] Z. H. Wang, Q. Zheng, Xiaoguang Wang and Yong Li, *Sci. Rep.* **6**, 22347 (2016).
 - [39] A. Joshi and S. V. Lawande, *Phys. Rev. A* **46**, 5906 (1992).
 - [40] M. J. Faghihi, M. K. Tavassoly and M. B. Harouni, *Laser Phys.* **24**, 045202 (2014).
 - [41] N. Imoto, H. A. Haus, Y. Yamamoto, *Phys. Rev. A* **32**, 2287 (1985).
 - [42] G. Berlin and J. Aliaga, *J. Mod. Opt.* **48**, 1819 (2001).
 - [43] R. Landauer, *Phys. Lett. A* **25**, 416 (1967).
 - [44] Y.-K. Yoon, R. S. Bennink, R. W. Boyd and J. E. Sipe, *Opt. Comm.* **179**, 577 (2000).
 - [45] S. A. Reyes, L. Morales-Molina, M. Orszag and D. Spehner, *E. Phys. Lett.* **108**, 20010 (2014).
 - [46] G. Vidal and R. F. Werner, *Phys. Rev. A* **65**, 032314 (2002).
 - [47] T. Baumgratz, M. Cramer and M. B. Plenio, *Phys. Rev. Lett.* **113**, 140401 (2014).
 - [48] A. Peres, *Phys. Rev Lett.* **77**, 1413 (1996).
 - [49] Y-C. Ou and H. Fan, *Phys. Rev. A* **75**, 062308 (2007).
 - [50] C. Sabin and G. Garcia-Alcaine, *Eur. Phys. J. D* **48**, 435 (2008).

- [51] F. Haake, “*Quantum Signature of Chaos*”, Springer, second edition (2001).
- [52] S. Sachdev, “*Quantum Phase Transitions*”, (Cambridge Univ. Press, 1999).
- [53] L. A. Wu, M. S. Sarandy and D. A. Lidar, Phys. Rev. Lett **93**, 250404 (2004).
- [54] S. Campbell, L. Mazzola, G. De Chiara, T. J. G. Apollaro, F. Plastina, Th. Busch and M. Paternostro, New J. Phys. **15**, 043033 (2013).
- [55] T. Werlang, C. Trippe, G. A. P. Ribeiro and G. Rigolin, Phys. Rev. Lett. **105**, 095702 (2010).
- [56] B. Schumacher, Phys. Rev. A **51**, 2738 (1995).
- [57] M. Orszag, *Quantum Optics*, Springer, 2nd edition (2008).
- [58] M. Orszag, N. Ciobanu, R. Coto and V. Ereemeev, J. Mod. Opt. **62**, 593 (2015).
- [59] R. Coto and M. Orszag, M. J. Phys. B: At. Mol. Opt. Phys. **46**, 175503 (2013).
- [60] M. J. Hartmann, F. G. S. L. Brandao and M. B. Plenio, Laser & Photon Rev. **2**, 527 (2008).
- [61] D. Underwood, W. Shanks, J. Koch, and A. A. Houck, Phys. Rev. A **86**, 023837 (2012).
- [62] H. Schmidt and A. Imamoglu, Opt. Lett. **21**, 1936 (1996).
- [63] M. J. Hartmann, F. G. S. L. Brandao and M. B. Plenio, Nature Phys. **2**, 849 (2006).
- [64] L. V. Hau, S. E. Harris, Z. Dutton, and C. H. Behroozi, Nature (London) **397**, 594 (1999).